THE JOURNAL OF PHYSICAL CHEMISTRY Letters

Letter

pubs.acs.org/JPCL

Revised Oxygen Evolution Reaction Activity Trends for First-Row Transition-Metal (Oxy)hydroxides in Alkaline Media

Michaela S. Burke,[†] Shihui Zou,[‡,†] Lisa J. Enman,[†] Jaclyn E. Kellon,[†] Christian A. Gabor,[†] Erica Pledger,[†] and Shannon W. Boettcher*[,†]

[†]Department of Chemistry and Biochemistry, 1253 University of Oregon, Eugene, Oregon 97403, United States

[‡]Key Lab of Applied Chemistry of Zhejiang Province, Department of Chemistry, Zhejiang University, Hangzhou, 310027, China

Supporting Information

ABSTRACT: First-row transition-metal oxides and (oxy)hydroxides catalyze the oxygen evolution reaction (OER) in alkaline media. Understanding the intrinsic catalytic activity provides insight into improved catalyst design. Experimental and computationally predicted activity trends, however, have varied substantially. Here we describe a new OER activity trend for nominally oxyhydroxide thin films of $Ni(Fe)O_xH_y$ > $Co(Fe)O_xH_y$ > FeO_xH_y-AuO_x > FeO_xH_y > CoO_xH_y > NiO_xH_y > MnO_xH_y. This intrinsic trend has been previously obscured by electrolyte impurities, potential-dependent electrical conductivity, and difficulty in correcting for surface-area or mass-loading differences. A quartz-crystal microbalance was used to monitor mass in situ and X-ray photoelectron spectroscopy to measure composition and impurity levels. These new results provide a basis for comparison to theory and help guide the design of improved catalyst systems.

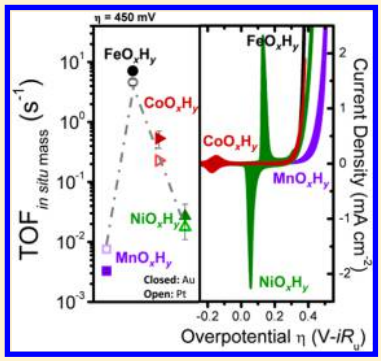

The slow kinetics of the oxygen evolution reaction (OER), in base, $4OH^- \rightarrow O_2 + 2H_2O + 4e^-$, and in acid, $2H_2O \rightarrow O_2 + 4H^+ + 4e^-$, limit the performance of large-scale energy technologies based on the photodriven or electricity-driven production of H_2 from water.[1−5] Development of improved catalysts can be accelerated by an enhanced understanding of the underlying electrocatalytic mechanism and its dependence on catalyst composition and structure. The paradigm for understanding heterogeneous OER catalysis that has emerged over a half-century of research is based on the application of the Sabatier principle.[6] The OER is thought to occur on a surface metal site, M, via a series of intermediates (e.g., M−OH, M−O, M−OOH, M−OO).[7] Because all of the intermediates are bound by an M−O bond, plotting activity versus the M−O bond strength should, in principle, result in an activity trend that forms a "volcano plot", where surfaces with either too-large or too-small M−O bond strengths are poor catalysts, as both lead to rate-determining steps with large activation energies.[7,8] Understanding OER catalysts based on earth-abundant first-row transition metals is of particular interest, as these catalysts might be used in water electrolysis or photoelectrolysis systems at a scale commensurate with global energy use. Consequently, there have been many experimental and computational efforts to correlate OER activity to chemical or material parameters.

Mn,[9−14] Fe,[15] Co,[16−18] and Ni-based[19] metal oxides and (oxy)hydroxides have been broadly studied and benchmarked for OER catalysis.[1,2,5,20] Early work by Delahay correlated the OER overpotential at 1 A cm^{-2} measured by Hickling[21] and the M−OH bond strength (with the metals in their highest oxidation states under the OER conditions).[22] The activity trend was Co ≈ Fe > Ni. Trasatti correlated the enthalpy of the reaction $MO_x + 1/2O_2 \rightarrow MO_{x+1}$ (which should reasonably correlate with the strength of the M−O bond) to the OER activity to generate a volcano relation with the precious metal oxides IrO_2 and RuO_2 at the top and the first-row transition metal oxides in the order MnO_2 > NiO > Co_3O_4 ≫ Fe_3O_4.[23,24] Lyons studied electrochemically conditioned metal electrodes and found an activity trend of Ni > Co > Fe.[25] A number of other studies have focused on perovskite oxides,[26,27] and correlated activity to the occupancy of the transition-metal e_g orbital,[28] which can also be related to the M−O bond strength.[29] Other experimental benchmarking studies have found activities of NiO_xH_y ≈ CoO_xH_y for electrodeposited (oxy)hydroxides.[30,31] Substantial variation among the reported activity trends is thus evident.

One limitation of many analyses is that differences in microscopic surface area and electrical conductivity of the catalyst layer are not well accounted for.[32−34] The use of thin-film electrodes with low loading, in principle, minimizes these confounding effects.[2] Subbaraman deposited near-monolayer (oxy)hydroxide films on single-crystal Pt and found activities of NiO_xH_y > CoO_xH_y > FeO_xH_y > MnO_xH_y,[35] which was correlated with the "oxophilicity" of the metal (i.e., M−O bond strength). Ni (oxy)hydroxide was thus assumed to have the most-optimal M−O bond strength among the first-row transition metals. We studied metal oxides in thin-film form and found the same activity trend and also that NiO was chemically unstable and transformed into (nominally) NiOOH,

Received: July 30, 2015
Accepted: September 2, 2015
Published: September 2, 2015

DOI: 10.1021/acs.jpclett.5b01650
J. Phys. Chem. Lett. 2015, 6, 3737−3742

which absorbed Fe impurities from the electrolyte during OER.[36] Studies in rigorously Fe-free electrolyte show Fe dramatically enhances activity and that pure NiOOH is a very poor OER catalyst,[37,38] consistent with the original studies by Corrigan.[19] Similar, but less dramatic, effects were found for Fe in CoOOH.[39] In an experimental/computational study, Friebel concluded that Fe is the active site for OER in the Ni(Fe)OOH system.[40]

Computational analyses using density functional theory (DFT) have also yielded varied results. Most work has focused on comparing different crystal faces and structures for single and mixed-cation oxides/(oxy)hydroxides of Co,[41−43] Co−Ni,[44] Mn,[45] and Ni/Ni−Fe,[40,46] oxides, and (oxy)hydroxides. In two cases, the analyses have been extended to include compositional/periodic activity trends. Man studied different crystalline phases and found that Co_3O_4 > NiO > Mn_xO_y ≈ NiOb (where NiOb is a different surface construction).[8] Calle-Vallejo studied MO surfaces and found NiO ≫ CoO ≈ FeO ≫ MnO.[47]

The lack of consistency among the various experimental and computational activity trends illustrates the fundamental challenge in understanding heterogeneous OER catalysis and appropriately applying the Sabatier principle. While "bulk" crystalline structures can easily be characterized, the active surface phases responsible for OER cannot. Most OER catalysts have been presumed to be oxides, but oxides are generally *not thermodynamically stable* in water relative to hydroxides and oxyhydroxides,[48−50] which is consistent with recent observations of structural changes in oxide OER catalysts.[36,51,52] The local chemical structure (protonation state, coordination geometry, oxidation state) of these hydrated, electrolyte-permeable phases further depends on the electrochemical potential and the electrolyte. Electrochemical polarization likely changes the catalyst structure and hence the M−O bond energy. Identifying and understanding activity trends is further complicated by the role of Fe impurities in OER, which appear to be widely present in even the highest-purity alkaline electrolytes that have not been specially purified[19,37,39] and the fact that the electrical conductivity widely varies among oxides and (oxy)hydroxides.[39,53,54] These issues raise significant concern regarding previous activity trends and their mechanistic interpretation.

Here we report a new activity trend for OER catalysts based on first-row transition metals that is different from previous experimental and computational trends. The catalysts are synthesized as thin films (with loading of ∼10 μg cm^{-2}) via electrodeposition at room temperature to directly access the hydrated oxide or (oxy)hydroxide phases that would otherwise form in situ at the surface of oxide-based catalysts synthesized at high temperature. Measurements are made on Au and Pt quartz-crystal-microbalance (QCM) electrodes, where the mass of the film is precisely quantified. Interdigitated electrodes are used to measure the electrical conductivity in situ of each catalyst and determine whether the measured activities are affected by poor electronic transport. All activity trends are reported as effective turnover frequencies (TOF, i.e., O_2 generated per second per metal cation) based on the total mass of the catalyst film calculated from the QCM measurement, assuming a formula weight of MOOH and that every metal cation is a possible active site (which is unlikely in the mixed metal cases). Nonetheless, we argue this is the most-consistent way to compare activity across a range of compositions; especially in the case of the porous, electrolyte-permeated (oxy)hydroxide-phase thin-film catalysts, where most metal cations are electrochemically accessible (see discussion below).

The dependence of TOF on overpotential, η, is shown in Figure 1A. The resulting activity trends for catalysts across the

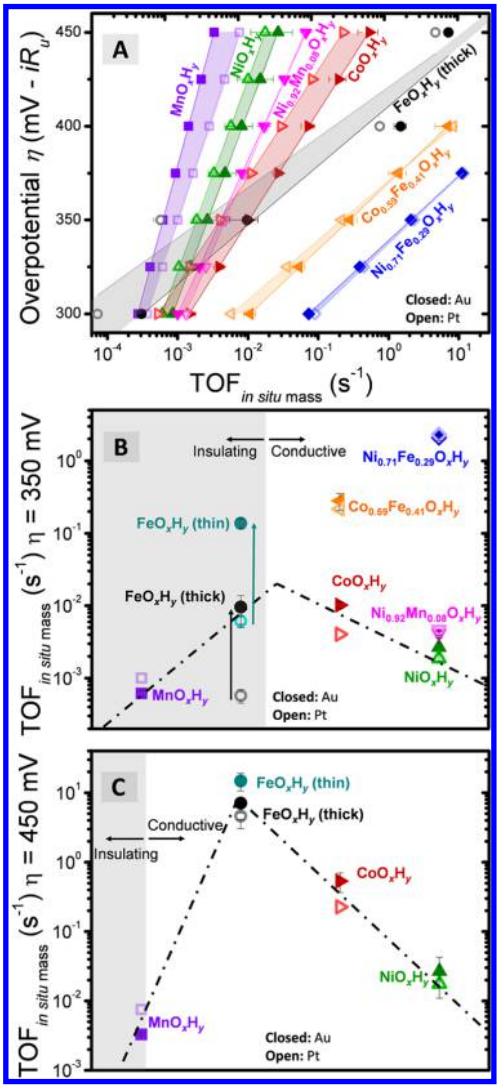

Figure 1. Activity analysis (A) as a function of overpotential, (B) at η = 350 mV, and (c) at η = 450 mV. The catalysts are synthesized by electrodeposition as (oxy)hydroxides on Au (closed symbols) and Pt (open symbols) microbalance electrodes and measured in triplicate for those on Au. (Some error bars are smaller than the symbols.) Compositions listed in (B) and (C) are ordered based on the atomic number of the host/primary cation. The fit lines and shading in (A) were added to make trends clear. The dotted lines in (B) and (C) are to guide the eye. Film masses were 8−12 μg cm^{-2} for all films except the thin FeO_xH_y which was 0.5 to 1.0 μg cm^{-2}. Exact masses can be found in Table S1. Because FeO_xH_y films slowly dissolve in 1 M KOH, measurements of FeO_xH_y were performed on different films at short time intervals where the film mass was constant.

first row of the transition metals are given in Figure 1B (η = 350 mV) and Figure 1C (η = 450 mV). Figure 2A shows the voltammetry of each film, while Figure 2B,C shows the conductivity measured in situ and the Tafel slopes from the best-fit lines in Figure 1A, respectively. All compositions are given by their stoichiometric ratios with a generalized (oxy)hydroxide formula so as not to specify any given oxidation

DOI: 10.1021/acs.jpclett.5b01650
J. Phys. Chem. Lett. 2015, 6, 3737−3742

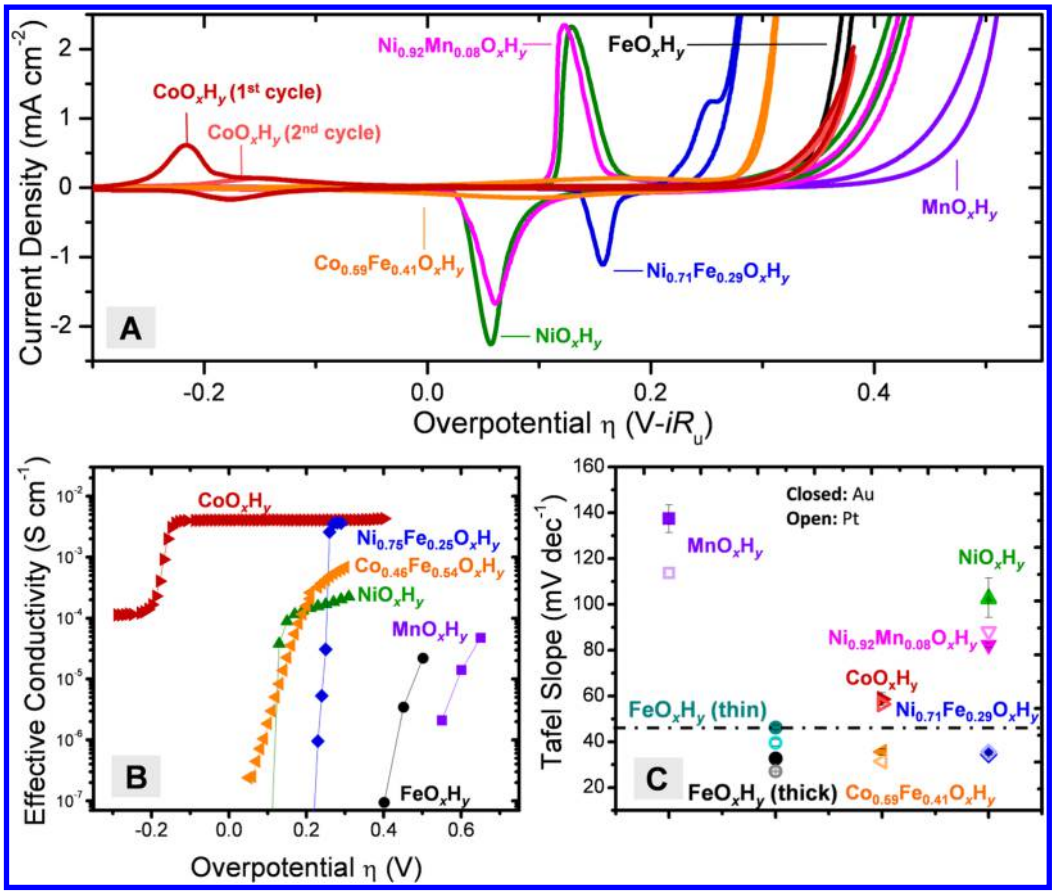

Figure 2. (A) Voltammetry of catalysts (10 mV s^{-1}) in 1 M KOH, (B) effective electrical conductivity, and (C) Tafel slopes extracted from the data in Figure 1A (closed symbols are on Au electrodes and open symbols are on Pt). The conductivity data in (B) for Co, Ni, Fe, and mixed Fe (oxy)hydroxides was previously published elsewhere,[37,39] and Mn conductivity was measured in 1 M KOH without rigorous cleaning of Fe impurities. The lowest conductivity points noted for FeO_xH_y and MnO_xH_y are the noise limit for the measurement on that sample. The dotted line in (C) marks the Tafel slope of FeO_xH_y measured on Au.

state. The compositions listed in the Figures were measured by XPS on Au substrates unless otherwise noted. Compositions measured on Pt for the mixed-metal catalysts are similar and are listed in Table S1.

These TOF data show that $Ni(Fe)O_xH_y$ has the highest OER activity at all the overpotentials studied, while $Co(Fe)O_xH_y$ has the second highest. Among the single-element (oxy)hydroxides the trend depends on the applied overpotential. At a high overpotential of 450 mV, the observed activity trend is FeO_xH_y > CoO_xH_y > NiO_xH_y > MnO_xH_y, independent of substrate (e.g., Au or Pt). At a lower overpotential of 350 mV, however, the activity of the FeO_xH_y depends strongly on the substrate and film thickness, which we attribute to the electronically insulating nature of FeO_xH_y at overpotentials below ~400 mV.[39] At 350 mV the majority of the FeO_xH_y film is electrically isolated and thus inactive. Thin FeO_xH_y films show much higher per-metal activity than thick films because a larger fraction of the Fe sites are electronically in contact with the underlying conductive Au or Pt. This is consistent with our observation that the substrate (Au or Pt) also affects the apparent activity of FeO_xH_y at η = 350 mV. The Fe sites strongly interacting with the metal support are those "electronically wired" and capable of driving OER. The strong activity enhancement on Au is consistent with the results of others on Co, Ni, and Mn (oxy)hydroxide ultrathin film OER catalysts on Au.[55−57] At η = 450 mV, FeO_xH_y becomes electronically conductive and a larger fraction of film (i.e., Fe sites further from the conducting Au or Pt) is likely to contribute to the observed activity. These data are thus consistent with the hypothesis that the poor electrical conductivity of the pure FeO_xH_y has prevented accurate measurement of the intrinsic OER activity of Fe sites in typically studied thick films or powder samples.[39] At η = 450 mV, the thin film of FeO_xH_y on Au retains a slightly higher TOF than its thick counterpart, but FeO_xH_y on Pt has a statistically identical TOF for both the thick and thin films, suggesting that FeO_xH_y on Pt shows its intrinsic TOF without substantial substrate enhancement.

Like FeO_xH_y, MnO_xH_y also shows OER activity that is only significant at overpotentials >400 mV, potentials near where the electrical conductivity becomes measurable (Figure 2B). When Fe is present within the electrically conductive NiO_xH_y or CoO_xH_y scaffolds, very high activity is observed, which has been tentatively attributed to "electronically wired" Fe active sites.[39,40] Besides the electronic connectivity, on a per-Fe-site basis, it appears that the "scaffolded" Fe is enhanced beyond that of FeO_xH_y on Pt or Au, even at higher overpotentials. This suggests a synergistic interaction between Fe and the Ni or Co cations. For catalysts that contain putative Fe active sites, the trend is thus $Ni(Fe)O_xH_y$ > $Co(Fe)O_xH_y$ > FeO_xH_y-AuO_x > FeO_xH_y-PtO_x. (Note that we indicate in this series that the surface of the Au or Pt electrode is probably oxidized under these conditions.) When Mn is coelectrodeposited with Ni to form $Ni(Mn)O_xH_y$, the resulting catalyst has similar activity to

DOI: 10.1021/acs.jpclett.5b01650
J. Phys. Chem. Lett. 2015, 6, 3737−3742

pure NiO_xH_y (Figure 1B), suggesting that the MnO_xH_y, in addition to being a poor electronic conductor, is an intrinsically poor OER catalyst compared with the Fe-based systems.

Cyclic voltammetry shows that the addition of Fe into Ni- and Co-(oxy)hydroxide anodically shifts both the $Co^{2+/3+}$ and $Ni^{2+/3+}$ redox waves (Figure 2A), indicating strong electronic interaction between the cations. It is interesting that the addition of Mn into NiO_xH_y does not induce a similar peak shift,[58] although we do note a difference in the cathodic peak integrated intensity and shape that is not understood at this point but is presumably also due to interactions between the cations. It is also possible to use the integrated redox peak areas for the Ni and Co (oxy)hydroxides to estimate the electrochemically active fraction of the films in conjunction with the QCM measurement (under appropriate conditions, see Burke et al.[39]). The Fe and Mn films do not have readily apparent redox features that can be used for this purpose; however, given that all of the films were deposited via an identical cathodic electroprecipitation as thin films, there is unlikely to be dramatic differences in electrolyte accessible surface area and the calculation of TOF based on the total metal sites is thus appropriate.

We note, however, that the apparent number of active Co and Ni sites appear to vary significantly in the voltammetry data shown. This is in part because the number of redox-active sites measured at steady-state during voltammetry is lower than that measured on the first cycle (as shown in Figure 2A for CoO_xH_y) due to the conductivity switching behavior of the films and the trapping of a portion of the film in the oxidized state (discussed in more detail in ref 39). After taking this effect into account, we estimate that the number of electrochemically accessible cations in the NiO_xH_y films is only about twice that of the CoO_xH_y films. While we could, in principle, correct the mass-based TOF data for this effect, we argue that such differences are small relative to the error inherent in estimating TOF and that the QCM mass-based TOF (per metal cation) remains the most-useful simple metric for comparison over a range of (oxy)hydroxide compositions.

We also note that Fe and Fe-mixed oxyhydroxides have the lowest Tafel slopes (Figure 2C). This suggests that the addition of Fe into the CoO_xH_y or NiO_xH_y host is a major factor in determining the rate-limiting step of the reaction.

Because the measurements were made on QCM electrodes, we also monitored the mass of the catalyst during all measurements. Figure 3 shows that all of the Ni- and Co-based catalysts (with or without Fe) were stable upon polarization, while FeO_xH_y dissolved substantially during the entire analysis and MnO_xH_y slightly at high current densities (5 ± 3% of mass). It is interesting to note that FeO_xH_y is the most active of the first-row transition-metal (oxy)hydroxides and also the most soluble, consistent with the activity-stability correlation found for noble OER catalysts in acid,[59] although the high stability and activity of the bimetallic $Ni(Fe)O_xH_y$ indicates that the correlation is not universal. Despite the high rate of dissolution for the FeO_xH_y, the corrosion current associated with the mass loss (assuming a possible $3e^-$ oxidation of FeOOH to soluble FeO_4^{2-}) would be <10% of the OER current at η = 300 mV and <0.3% of the OER current at η = 350 mV.

While it is tempting to plot the activity trends versus a chemical descriptor, this is particularly challenging with the materials under study. We find that good OER catalysts are also electrical conductors in their active state, suggesting the

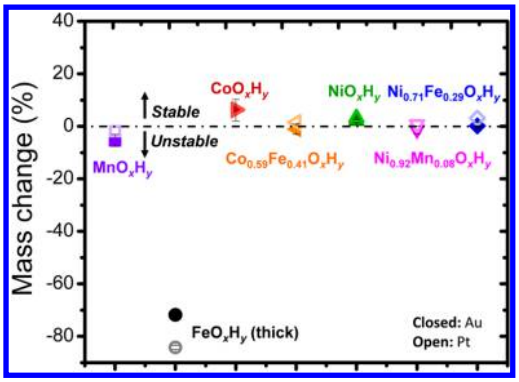

Figure 3. Mass changes after steady-state Tafel analysis. The Tafel analysis was performed at current densities between 10^{-5} and 10^{-2} A cm^{-2} (see SI for data) in 12 steps (total 53 min). Closed symbols are on Au electrodes and open symbols are on Pt. Several points overlap. The small mass gains for the CoO_xH_y catalysts are due to anodic electrodeposition of Co ions from the electrolyte which was cleaned of Fe impurities using CoO_xH_y powders.

electronic structure is delocalized and likely band-like. The cations are thus unlikely to have integer oxidation states during OER, which makes, for example, counting the e_g electrons difficult. Furthermore, the effective oxidation state is likely a function of overpotential. In the Figures above we have simply plotted the cations in order of increasing atomic number.

In conclusion, these new measurements provide a clear activity trend for the first-row transition metals that can be interpreted in the absence of confounding surface area, conductivity, and Fe-impurity affects. The data explain why FeO_xH_y catalysts are typically not considered to be good at the OER (low electrical conductivity) and why Ni-based catalysts are often found at the top of experimental volcano curves (Fe impurities). In basic media, MnO_xH_y is neither a good OER catalyst nor a good electrical conductor. These data should thus help in benchmarking improved computational methods that can accurately compare the activities of the hydrated (oxy)-hydroxide OER-active catalysts as well as guide experimental catalyst design efforts.

■ ASSOCIATED CONTENT

Supporting Information

The Supporting Information is available free of charge on the ACS Publications website at DOI: 10.1021/acs.jpclett.5b01650.

Experimental methods, tabulated data from figures, additional data, and discussion of Fe contamination in MnO_xH_y, and substrate enhancement effects. Cyclic voltammograms of the films before and after activity analysis. Tafel analyses, in situ mass measurements, XP spectra, and SEM images for each material. (PDF)

■ AUTHOR INFORMATION

Corresponding Author

*E-mail: swb@uoregon.edu.

Notes

The authors declare no competing financial interest.

■ ACKNOWLEDGMENTS

This work was supported by the National Science Foundation through CHE-1301461. S.Z. acknowledges the China Scholar Council for financial support. We thank Dr. Adam M. Smith,

DOI: 10.1021/acs.jpclett.5b01650
J. Phys. Chem. Lett. 2015, 6, 3737−3742

Matt G. Kast, Dr. Lena Trotochaud, and Adam Batchellor for insightful discussion. We acknowledge Dr. Stephen Golledge for help with XPS data interpretation. The project made use of CAMCOR facilities supported by grants from the W. M. Keck Foundation, the M. J. Murdock Charitable Trust, ONAMI, the Air Force Research Laboratory (FA8650-05-1-5041), the National Science Foundation (0923577 and 0421086), and the University of Oregon. S.W.B. thanks the Research Corporation for Science Advancement, the Sloan Foundation, and the Camille and Henry Dreyfus Foundation for additional support.

REFERENCES

(1) Walter, M. G.; Warren, E. L.; McKone, J. R.; Boettcher, S. W.; Mi, Q.; Santori, E. A.; Lewis, N. S. Solar Water Splitting Cells. *Chem. Rev.* **2010**, *110*, 6446−6473.
(2) Trotochaud, L.; Boettcher, S. W. Precise Oxygen Evolution Catalysts: Status and Opportunities. *Scr. Mater.* **2014**, *74*, 25−32.
(3) Mckone, J. R.; Lewis, N. S.; Gray, H. B. Will Solar-Driven Water-Splitting Devices See the Light of Day? *Chem. Mater.* **2014**, *26*, 407−414.
(4) Lewis, N. S.; Nocera, D. G. Powering the Planet: Chemical Challenges in Solar Energy Utilization. *Proc. Natl. Acad. Sci. U. S. A.* **2006**, *103*, 15729−15735.
(5) Galán-Mascarós, J. R. Water Oxidation at Electrodes Modified with Earth-Abundant Transition-Metal Catalysts. *ChemElectroChem* **2015**, *2*, 37−50.
(6) Sabatier, F. *La Catalyse En Chimie Organique*; Berauge: Paris, 1920.
(7) Rossmeisl, J.; Qu, Z.-W.; Zhu, H.; Kroes, G.-J.; Nørskov, J. K. Electrolysis of Water on Oxide Surfaces. *J. Electroanal. Chem.* **2007**, *607*, 83−89.
(8) Man, I. C.; Su, H. Y.; Calle-Vallejo, F.; Hansen, H. a.; Martínez, J. I.; Inoglu, N. G.; Kitchin, J.; Jaramillo, T. F.; Nørskov, J. K.; Rossmeisl, J. Universality in Oxygen Evolution Electrocatalysis on Oxide Surfaces. *ChemCatChem* **2011**, *3*, 1159−1165.
(9) Indra, A.; Menezes, P. W.; Sahraie, N. R.; Bergmann, A.; Das, C.; Tallarida, M.; Schmeißer, D.; Strasser, P.; Driess, M. Unification of Catalytic Water Oxidation and Oxygen Reduction Reactions: Amorphous Beat Crystalline Cobalt Iron Oxides. *J. Am. Chem. Soc.* **2014**, *136*, 17530−17536.
(10) Huynh, M.; Bediako, D. K.; Liu, Y.; Nocera, D. G. *J. Phys. Chem. C* **2014**, *118*, 17142−17152.
(11) Pickrahn, K. L.; Park, S. W.; Gorlin, Y.; Lee, H. B. R.; Jaramillo, T. F.; Bent, S. F. Active MnO_x Electrocatalysts Prepared by Atomic Layer Deposition for Oxygen Evolution and Oxygen Reduction Reactions. *Adv. Energy Mater.* **2012**, *2*, 1269−1277.
(12) Gorlin, Y.; Lassalle-kaiser, B.; Benck, J. D.; Gul, S.; Webb, S. M.; Yachandra, V. K.; Yano, J.; Jaramillo, T. F. In Situ X-Ray Absorption Spectroscopy Investigation of a Bifunctional Manganese Oxide Catalyst with High Activity for Electrochemical Water Oxidation and Oxygen Reduction. *J. Am. Chem. Soc.* **2013**, *135*, 8525−8534.
(13) Lutterman, D. A.; Surendranath, Y.; Nocera, D. G. A Self-Healing Oxygen-Evolving Catalyst. *J. Am. Chem. Soc.* **2009**, *131*, 3838−3839.
(14) Robinson, D. M.; Go, Y. B.; Mui, M.; Gardner, G.; Zhang, Z.; Mastrogiovanni, D.; Garfunkel, E.; Li, J.; Greenblatt, M.; Dismukes, G. C. Photochemical Water Oxidation by Crystalline Polymorphs of Manganese Oxides: Structural Requirements for Catalysis. *J. Am. Chem. Soc.* **2013**, *135*, 3494−3501.
(15) Wu, Y.; Chen, M.; Han, Y.; Luo, H.; Su, X.; Zhang, M.-T.; Lin, X.; Sun, J.; Wang, L.; Deng, L.; et al. Fast and Simple Preparation of Iron-Based Thin Films as Highly Efficient Water-Oxidation Catalysts in Neutral Aqueous Solution. *Angew. Chem., Int. Ed.* **2015**, *54*, 4870−4875.
(16) Klingan, K.; Ringleb, F.; Zaharieva, I.; Heidkamp, J.; Chernev, P.; Gonzalez-Flores, D.; Risch, M.; Fischer, A.; Dau, H. Water Oxidation by Amorphous Cobalt-Based Oxides: Volume Activity and Proton Transfer to Electrolyte Bases. *ChemSusChem* **2014**, *7*, 1301−1310.
(17) Surendranath, Y.; Kanan, M. W.; Nocera, D. G. Mechanistic Studies of the Oxygen Evolution Reaction by a Cobalt-Phosphate Catalyst at Neutral pH. *J. Am. Chem. Soc.* **2010**, *132*, 16501−16509.
(18) Kanan, M. W.; Nocera, D. G. In Situ Formation of an Oxygen-Evolving Catalyst in Neutral Water Containing Phosphate and Co^{2+}. *Science* **2008**, *321*, 1072−1075.
(19) Corrigan, D. A. The Catalysis of the Oxygen Evolution Reaction by Iron Impurities in Thin Film Nickel Oxide Electrodes. *J. Electrochem. Soc.* **1987**, *134*, 377−384.
(20) Singh, A.; Spiccia, L. Water Oxidation Catalysts Based on Abundant 1st Row Transition Metals. *Coord. Chem. Rev.* **2013**, *257*, 2607−2622.
(21) Hickling, A.; Hill, S. Oxygen Overvoltage. Part I. The Influence of Electrode Material, Current Density, and Time in Aqueous Solution. *Discuss. Faraday Soc.* **1947**, *1*, 236.
(22) Ruetschi, P.; Delahay, P. Influence of Electrode Material on Oxygen Overvoltage - A Theoretical Analysis. *J. Chem. Phys.* **1955**, *23*, 556−560.
(23) Trasatti, S. Electrocatalysis in the Anodic Evolution Oxygen and Chlorine? *Electrochim. Acta* **1984**, *29*, 1503−1512.
(24) Trasatti, S. Electrocatalysis by Oxides — Attempt at a Unifying Approach. *J. Electroanal. Chem. Interfacial Electrochem.* **1980**, *111*, 125−131.
(25) Lyons, M. E. G.; Brandon, M. P. A Comparative Study of the Oxygen Evolution Reaction on Oxidised Nickel, Cobalt and Iron Electrodes in Base. *J. Electroanal. Chem.* **2010**, *641*, 119−130.
(26) Bockris, J. O. M.; Otagawa, T. The Electrocatalysis of Oxygen Evolution on Perovskites. *J. Electrochem. Soc.* **1984**, *131*, 290−302.
(27) Bockris, J. O.; Otagawa, T. Oxygen Evolution on Perovskites. *J. Phys. Chem.* **1983**, *87*, 2960−2971.
(28) Suntivich, J.; May, K. J.; Gasteiger, H. A.; Goodenough, J. B.; Shao-Horn, Y. A Perovskite Oxide Optimized for Oxygen Evolution Catalysis from Molecular Orbital Principles. *Science* **2011**, *334*, 1383−1385.
(29) Vojvodic, A.; Nørskov, J. K. Optimizing Perovskites for the Water-Splitting Reaction. *Science* **2011**, *334*, 1355−1356.
(30) McCrory, C. C. L.; Jung, S.; Peters, J. C.; Jaramillo, T. F. Benchmarking Heterogeneous Electrocatalysts for the Oxygen Evolution Reaction. *J. Am. Chem. Soc.* **2013**, *135*, 16977−16987.
(31) Merrill, M. D.; Dougherty, R. C. Metal Oxide Catalysts for the Evolution of O_2 from H_2O. *J. Phys. Chem. C* **2008**, *112*, 3655−3666.
(32) Trasatti, S. Physical Electrochemistry of Ceramic Oxides. *Electrochim. Acta* **1991**, *36*, 225−241.
(33) Trasatti, S.; Petrii, O. A. Real Surface Area Measurements. *J. Electroanal. Chem.* **1992**, *327*, 353−376.
(34) Ardizzone, S.; Trasatti, S. Interfacial Properties of Oxides with Technological Impact in Electrochemistry. *Adv. Colloid Interface Sci.* **1996**, *64*, 173−251.
(35) Subbaraman, R.; Tripkovic, D.; Chang, K.-C.; Strmcnik, D.; Paulikas, A. P.; Hirunsit, P.; Chan, M.; Greeley, J.; Stamenkovic, V.; Markovic, N. M. Trends in Activity for the Water Electrolyser Reactions on 3d M(Ni,Co,Fe,Mn) Hydr(oxy)oxide Catalysts. *Nat. Mater.* **2012**, *11*, 550−557.
(36) Trotochaud, L.; Ranney, J. K.; Williams, K. N.; Boettcher, S. W. Solution-Cast Metal Oxide Thin Film Electrocatalysts for Oxygen Evolution. *J. Am. Chem. Soc.* **2012**, *134*, 17253−17261.
(37) Trotochaud, L.; Young, S. L.; Ranney, J. K.; Boettcher, S. W. Nickel-Iron Oxyhydroxide Oxygen-Evolution Electrocatalysts: The Role of Intentional and Incidental Iron Incorporation. *J. Am. Chem. Soc.* **2014**, *136*, 6744−6753.
(38) Smith, A. M.; Trotochaud, L.; Burke, M. S.; Boettcher, S. W. Contributions to Activity Enhancement via Fe Incorporation in Ni-(oxy)hydroxide/borate Catalysts for Near-Neutral pH Oxygen Evolution. *Chem. Commun.* **2015**, *51*, 5261−5263.
(39) Burke, M. S.; Kast, M. G.; Trotochaud, L.; Smith, A. M.; Boettcher, S. W. Cobalt-Iron (oxy)hydroxide Oxygen Evolution

DOI: 10.1021/acs.jpclett.5b01650
J. Phys. Chem. Lett. 2015, 6, 3737−3742

Electrocatalysts: The Role of Structure and Composition on Activity, Stability, and Mechanism. *J. Am. Chem. Soc.* **2015**, *137*, 3638−3648.
(40) Friebel, D.; Louie, M. W.; Bajdich, M.; Sanwald, K. E.; Cai, Y.; Wise, A. M.; Cheng, M.-J.; Sokaras, D.; Weng, T.-C.; Alonso-Mori, R.; et al. Identification of Highly Active Fe Sites in (Ni,Fe)OOH for Electrocatalytic Water Splitting. *J. Am. Chem. Soc.* **2015**, *137*, 1305−1313.
(41) Chen, J.; Selloni, A. First Principles Study of Cobalt (Hydr)oxides under Electrochemical Conditions. *J. Phys. Chem. C* **2013**, *117*, 20002−20006.
(42) Friebel, D.; Bajdich, M.; Yeo, B. S.; Louie, M. W.; Miller, D. J.; Sanchez Casalongue, H.; Mbuga, F.; Weng, T.-C.; Nordlund, D.; Sokaras, D.; et al. On the Chemical State of Co Oxide Electrocatalysts during Alkaline Water Splitting. *Phys. Chem. Chem. Phys.* **2013**, *15*, 17460−17467.
(43) García-Mota, M.; Bajdich, M.; Viswanathan, V.; Vojvodic, A.; Bell, A. T.; Nørskov, J. K. Importance of Correlation in Determining Electrocatalytic Oxygen Evolution Activity on Cobalt Oxides. *J. Phys. Chem. C* **2012**, *116*, 21077−21082.
(44) Bajdich, M.; García-Mota, M.; Vojvodic, A.; Nørskov, J. K.; Bell, A. T. Theoretical Investigation of the Activity of Cobalt Oxides for the Electrochemical Oxidation of Water. *J. Am. Chem. Soc.* **2013**, *135*, 13521−13530.
(45) Busch, M.; Ahlberg, E.; Panas, I. Electrocatalytic Oxygen Evolution from Water on a Mn(III-V) Dimer Model Catalyst-a DFT Perspective. *Phys. Chem. Chem. Phys.* **2011**, *13*, 15069−15076.
(46) Li, Y.; Selloni, A. Mechanism and Activity of Water Oxidation on Selected Surfaces of Pure and Fe-Doped NiO_x. *ACS Catal.* **2014**, *4*, 1148−1153.
(47) Calle-Vallejo, F.; Diaz-Morales, O.; Kolb, M.; Koper, M. T. M. Why Is Bulk Thermochemistry a Good Descriptor for the Electrocatalytic Activity of Transition Metal Oxides? *ACS Catal.* **2015**, *5*, 869−873.
(48) Schweitzer, G. K.; Pesterfield, L. L. *The Aqueous Chemistry of the Elements*; Oxford University Press: Oxford, U.K., 2010.
(49) Pourbaix, M. *Atlas of Electrochemical Equilibria in Aqueous Solutions*; Pergamon Press: Oxford, U.K., 1966.
(50) Binninger, T.; Mohamed, R.; Waltar, K.; Fabbri, E.; Levecque, P.; Kötz, R.; Schmidt, T. J. Thermodynamic Explanation of the Universal Correlation between Oxygen Evolution Activity and Corrosion of Oxide Catalysts. *Sci. Rep.* **2015**, *5*, 12167.
(51) May, K. J.; Carlton, C.; Stoerzinger, K. A.; Risch, M.; Suntivich, J.; Lee, Y.; Grimaud, A.; Shao-horn, Y. Influence of Oxygen Evolution during Water Oxidation on the Surface of Perovskite Oxide Catalysts. *J. Phys. Chem. Lett.* **2012**, *3*, 3264−3270.
(52) Risch, M.; Grimaud, A.; May, K. J.; Stoerzinger, K. A.; Chen, T. J.; Mansour, A. N.; Shao-Horn, Y. Structural Changes of Cobalt-Based Perovskites upon Water Oxidation Investigated by EXAFS. *J. Phys. Chem. C* **2013**, *117*, 8628−8635.
(53) Viswanathan, V.; Pickrahn, K. L.; Luntz, A. C.; Bent, S. F.; Nørskov, J. K. Nanoscale Limitations in Metal Oxide Electrocatalysts for Oxygen Evolution. *Nano Lett.* **2014**, *14*, 5853−5857.
(54) Klaus, S.; Cai, Y.; Louie, M. W.; Trotochaud, L.; Bell, A. T. Effects of Fe Electrolyte Impurities on $Ni(OH)_2$/NiOOH Structure and Oxygen Evolution Activity. *J. Phys. Chem. C* **2015**, *119*, 7243−7254.
(55) Yeo, B. S.; Bell, A. T. Enhanced Activity of Gold-Supported Cobalt Oxide for the Electrochemical Evolution of Oxygen. *J. Am. Chem. Soc.* **2011**, *133*, 5587−5593.
(56) Yeo, B. S.; Klaus, S. L.; Ross, P. N.; Mathies, R. A.; Bell, A. T. Identification of Hydroperoxy Species as Reaction Intermediates in the Electrochemical Evolution of Oxygen on Gold. *ChemPhysChem* **2010**, *11*, 1854−1857.
(57) Frydendal, R.; Busch, M.; Halck, N. B.; Paoli, E. A.; Krtil, P.; Chorkendorff, I.; Rossmeisl, J. Enhancing Activity for the Oxygen Evolution Reaction: The Beneficial Interaction of Gold with Manganese and Cobalt Oxides. *ChemCatChem* **2015**, *7*, 149−154.
(58) Corrigan, D. A.; Bendert, R. M. Effect of Coprecipitated Metal Ions on the Electrochemistry of Nickel Hydroxide Thin Films: Cyclic Voltammetry in 1M KOH. *J. Electrochem. Soc.* **1989**, *136*, 723−728.
(59) Danilovic, N.; Subbaraman, R.; Chang, K.; Chang, S. H.; Kang, Y. J.; Snyder, J.; Paulikas, A. P.; Strmcnik, D.; Kim, Y.; Myers, D.; et al. Activity − Stability Trends for the Oxygen Evolution Reaction on Monometallic Oxides in Acidic Environments. *J. Phys. Chem. Lett.* **2014**, *5*, 2474−2478.

DOI: 10.1021/acs.jpclett.5b01650
J. Phys. Chem. Lett. 2015, 6, 3737−3742